Geomechanics and Engineering, *Vol. 38, No. 1 (2024) 45-56*
https://doi.org/10.12989/gae.2024.38.1.045

Mechanical damage evolution and a statistical damage constitutive model for water-weak sandstone and mudstone

Lu yuan Wu*[1], Fei Ding[1], Jian hui Li[1] and Wei Qiao[2]

[1]*School of Civil Engineering and Architecture, Henan University, Jin ming Street, Kaifeng, 475001, Henan, China.*
[2]*School of Resources and Earth Sciences, China University of Mining and Technology, Xuzhou, 221116, Jiangsu, China*

(*Received September 5, 2023, Revised June 16, 2024, Accepted June 26, 2024*)

Abstract. The weakening effect of water on rocks is one of the main factors inducing deformation and failure in rock engineering. To clarify this weakening effect, immersion tests and post-immersion triaxial compression tests were conducted on sandstone and mudstone. The results showed that the strength of water-immersed sandstone decreases with increasing immersion time, exhibiting an exponential relationship. Similarly, the strength of water-immersed mudstone decreases with increasing environmental humidity, also following an exponential relationship. Subsequently, a statistical damage model for water-weakened rocks was proposed, changes in elastic modulus to describe the weakening effect of water. The model effectively simulated the stress-strain relationships of water-affected sandstone and mudstone under compression. The R^2 values between the theoretical and experimental peak values ranged from 0.962 to 0.996, and the MAPE values fell between 3.589% and 9.166%, demonstrating the model's effectiveness and reliability. The damage process of water-saturated rocks corresponds to five stages: compaction stage - no damage, elastic stage - minor damage, crack development stage - rapid damage increase, post-peak residual stage - continuous damage increase, and sliding stage - damage completion. This study provides a foundational reference for researching the fracture characteristics of overlying strata during coal mining under complex hydrogeological conditions.

Keywords: ambient humidity; immersion time; rock constitutive model; rock damage; water-weak

1. Introduction

Rocks are natural material which mechanical properties exert a pivotal influence on construction and production activities. Nevertheless, the mechanical properties of rocks are shaped not only by internal factors, including mineral composition, microstructure, and the type of bonding between rock grains (Mousavi *et al.* 2020a, Wu *et al.* 2020, He *et al.* 2019, Peng 2018, Sun *et al.* 2023), but also by external environmental factors, most notably the impact of groundwater (Yang *et al.* 2011). Water can affect the deformation and strength characteristics of rocks, leading to a certain degree of weakening of their mechanical performance (Li *et al.* 2015), which is a causative factor in various geological disasters, such as landslides (Miao *et al.* 2022) and mine collapse (Ma *et al.* 2018). In recent years, the study of the strength failure mechanism of rock under water-bearing conditions has become a hot topic (Xie *et al.* 2022). Previous research has thoroughly demonstrated that the compressive strength of rocks will exhibit varying degrees of decline under the influence of water (Kim *et al.* 2017, Mousavi *et al.* 2020b). Furthermore, Pan *et al.* (2022) and Qi *et al.* (2022) have also elucidated that water can alter the chemical composition of rocks and influence their microstructure, thereby changing their properties. Therefore, a comprehensive understanding of the impact of water on rocks is crucial for assessing their durability and strength. (Bian *et al.* 2019).

Numerous scholars have investigated the impact of water-weakening on rocks(Liu *et al.* 2023, Huang *et al.* 2008, Zhang *et al.* 2013, Wang *et al.* 2020, Shi *et al.* 2016, Olena 2019, Zhang *et al.* 2023, Cai *et al.* 2019, Zhang *et al.* 2022), discovering that the degree of rock strength degradation caused by water is influenced by the physical characteristics, initial condition, water content, density, and stress status of the rock, as well as environmental factors, such as freeze-thaw conditions (Seyed *et al.* 2020, Mousavi and M 2022, Zhai *et al.* 2022). Moreover, there is also a significant correlation with the type of rock There are significant differences between various rock classes (Wasantha and Ranjith 2014).

When rocks are subjected to external forces (including water-induced weakening), microcracks gradually nucleate and propagate, eventually leading to the formation of macroscopic cracks and ultimately, rock failure. This process is a cumulative damage process that ultimately culminates in rock failure, hence the introduction of damage mechanics. The investigation of rock damage mechanics mainly entails investigating damage mechanisms, developing damage models, and analyzing the complete progression of damage development: from micro-scale fracture to macro-scale fracture. The establishment of the rock's constitutive equation and the exploration of its damage mechanisms are the primary concerns of the damage theory(Jean Lemaitre and Chunhu 1996).

*Corresponding author, Professor
E-mail: wulymp@henu.edu.cn

ISSN: 2005-307X (Print), 2092-6219 (Online)

Researchers establish the damage equation and determine the degree of damage to predict the remaining life of rocks or evaluate the stability of the medium. Presently, statistical damage mechanics offers innovative ideas and approaches to explore the mechanical properties of rock materials and engineering (Qin 2001), and the statistical damage master equation is widely recognized as an effective tool for analyzing rock damage processes.

Since Krajcinovic and Silva (1982) proposed the concept of a statistical damage intrinsic model for rocks, and Rabotnov (1963) and Kachanov introduced the concept of damage and damage factors, scholars have conducted extensive research on damage constitutive models, achieving numerous breakthroughs, such as the temperature damage model(Wang *et al.* 2022, Zhang *et al.* 2022, Liu *et al.* 2021) and the freeze-thaw damage model(Chen *et al.* 2021, Yang and Jiang 2022, Mousavi *et al.* 2019). However, research on the destructive effect of water on rocks is currently very limited (Ma *et al.* 2016). He *et al.* (2019) put forward a statistical damage model for rocks under water pressure based on the Hoek-Brown strength criterion, which is modified to reflect the deformation characteristics of rocks under water pressure. Xtfa *et al.* (2001) conducted experiments to investigate the deterioration of granite's mechanical properties caused by water chemical corrosion. The study yielded a set of damage variables and corresponding constitutive relationships for the rock. However, these analyses only demonstrate the pressure effect of water, the deformation characteristics of rocks, and the impact of hydrochemical processes on rocks, failing to effectively address the comprehensive weakening effects of water on rocks and neglecting to validate the entire process of water induced damage. In this context, establishing a statistical damage constitutive model that considers the water weakening effect will provide a new avenue for analyzing the impact of water-induced damage on the mechanical behavior of rocks.

To accurately determine the changes in rock mechanical parameters during the water-rock interaction process, rock mechanical experiments are an indispensable method. For instance, Bian *et al.* (2019) proposed a damage constitutive model for a rock exposed to water-weakening effects (soaking rock) through indoor experiments; however, the model is considered unsuitable for disaggregated rock, such as mudstone. Moreover, many scholars have investigated the effects of water chemical corrosion on rocks, such as Zhou *et al.* (2017), who conducted uniaxial and triaxial compression tests to examine the strength softening and deformation of gypsum rock under natural and saturated conditions. Similarly, Li *et al.* (2020) studied the impact of mineral components on rock-water interaction through X-ray diffraction and water absorption tests under dry, wet, and saturated states of shale. However, their research on the combined effects of chemical corrosion, water, and confining pressure on rock damage is insufficient, particularly in terms of constitutive modeling.

Based on the aforementioned research, this study first investigates the variation patterns of mechanical properties of sandstone and mudstone under different soaking times and environmental humidity conditions through triaxial compression tests. Building on the Lemaitre strain equivalence hypothesis, the D-P criterion, and damage mechanics theory, a rock damage model is established that accounts for the water weakening effect and triaxial loading. The theoretical curves exhibit good agreement with the experimental data, accurately reflecting the stress-strain characteristics and strength variation patterns of rocks, thereby validating the rationality and feasibility of the model.

2 Establishment of statistical damage constitutive model

2.1 Statistical damage evolution equation based on statistical strength theory

It is assumed that N_i is the number of failed microelements of the rock under a certain load; N_{ni} is the number of unfailed (no damage) microelements, and the N is the total number of microelements. Then the statistical damage variable is defined as D, which is the ratio of the number of failed microelements to the total number of microelements, i.e.

$$D = \frac{N_{\mathrm{i}}}{N_{\mathrm{i}} + \mathrm{N}_{\mathrm{ni}}} \tag{1}$$

where D=0, corresponds to the no damage state, D=1 is corresponding to the complete damage (fracture state), $0 < D < 1$ is corresponding to different degrees of damage state.

$$D_{wd} = E(w,t) \tag{2}$$

Notably, the damage variable affected by water, $E(w, t)$, pertains to the water content and immersion time of the rock. Based on the rock's physical properties and damage characteristics, this paper establishes the damage model making the following assumptions:

(1) the rock damage is elastic and plastic damage is not considered;

(2) Rock damage is concentrated in the axial direction;

(3) The damage evolution equation is a function of the stress-strain state.

The guidelines on D-P strength can be summarized as follows

$$S - F = 0 \tag{3}$$

where S is the stress level and F is a constant, which indicates the material strength. When the stress level S in a micro-element reaches its strength F, the micro-element fails.

Assuming that each micro-element's strength F follows some probability distribution, the maximum value that the stress level S in each micro-element can reach also follows this same probability distribution. This relationship can be expressed as

$$F = P(x) \tag{4}$$

where P is the density function of the probability distribution satisfied by the microelement strength F and x represents the microelement strength of the rock.

2.2 Damage principal structure equation based on continuum damage mechanics

If the undamaged rock is a linear elastic material, then replacing the principal stress σ_i in Hooke's law of linear elasticity with the effective principal stress σ_i^* can obtain

$$\sigma_i = \sigma_i^*(1-D) \tag{5}$$

$$\varepsilon_i = \frac{1}{E}[(1+v)\sigma_i^* - v(\sigma_1^* + \sigma_2^* + \sigma_3^*)(1-D), \quad i=1,2,3 \tag{6}$$

where ε_i is the principal strain, E is the modulus of elasticity, and v is the Poisson's ratio.

Eq. (6) expresses the principal strains in three directions. In triaxial compression tests, the axial principal strain ε_1 is highly important and straightforward to measure, so this paper takes the free index i in Eq. (6) always as 1. Furthermore, when the second principal stress σ_2 is equal to the third principal stress σ_3, such as in triaxial compression tests of rocks, the circumferential pressures also become equal,meaning that σ_2 is equal to σ_3 (i.e., $\sigma_2 = \sigma_3$).

Combining Eqs. (5) and (6), the axial principal strain can be obtained as

$$\varepsilon_i = \frac{\sigma_1 - 2v\sigma_3}{E(1-D)} \tag{7}$$

Therefore, the expression of the damage variable is

$$D = 1 - \frac{\sigma_1 - 2v\sigma_3}{E\varepsilon_1} \tag{8}$$

As the development of micro-defects within the rock follows a random distribution pattern, it is crucial to consider the statistical damage theory to study this phenomenon. And the probability distributions are Weibull distribution, power function distribution, normal distribution, etc. Among them, Weibull distribution has achieved good results (Xu and Wei 2002, Cao *et al.* 1998). Therefore, the Weibull distribution is chosen, and its density function and distribution function are respectively

$$P(x) = \frac{m}{n}(\frac{x}{n})^{m-1}\exp[-(\frac{x}{n})^m] \tag{9}$$

$$P(x) = 1 - \exp[-(\frac{x}{n})^m] \tag{10}$$

where, m and n are statistical parameters.

Due to the inability of the M-C criterion to describe complete and hard homogeneous rock blocks, the D-P strength criterion is used in this paper to describe the strength of micro-elements and the expression of the D-P criterion is as follows

$$S = f(\sigma^*) = \sqrt{J_2^*} - \alpha I_1^* \tag{11}$$

where I_1^* is the first invariant of stress, and $J_2^*$is the second invariant of stressbias. For the triaxial compression test, the equivalent relation is $\sigma_2^* = \sigma_3^*$, which can be deduced as

$$\mathrm{I}_1^* = \sigma_1^* + \sigma_2^* + \sigma_3^* = \frac{E\varepsilon_1(\sigma_1 + 2v\sigma_3)}{\sigma_1 - 2v\sigma_3} \tag{12}$$

$$\sqrt{\mathrm{J}_2^*} = E\varepsilon_1(\sigma_1 - \sigma_3)/\sqrt{3}(\sigma_1 - 2v\sigma_3) \tag{13}$$

σ_i^* is the effective principal stress, and v is the Poisson's ratio. From Eqs. (3), (6), (11), (12), and (13), it follows that

$$S = \frac{E\varepsilon_1}{\sigma_1 - 2v\sigma_3}[\frac{1}{\sqrt{3}}(\sigma_1 - \sigma_3) - \alpha(\sigma_1 + 2\sigma_3)] \tag{14}$$

Several methods exist for determining the material parameter α. In the π-plane, the Mohr-Coulomb (M-C) criterion envelope has a hexagonal shape, while the D-P criterion envelope is circular. There are various methods for calculating the material parameter α. If the preset D-P criterion envelope and M-C criterion both qual areas(Wong 2013), the following equation can be used to calculate the parameter

$$\alpha = \sqrt{\frac{4\sqrt{3}\sin^2\phi}{2\pi(9-\sin^2\phi)}} \tag{15}$$

2.3 Statistical damage principal structure model

From Eqs. (3), (4), (8), (10) and (14), the statistical damage intrinsic model can be obtained as

$$\exp\left\{-\left\{\begin{matrix}\frac{E\varepsilon_1}{n(\sigma_1 - 2v\sigma_3)}[\frac{1}{\sqrt{3}}(\sigma_1 - \sigma_3)\\ -\alpha(\sigma_1 + 2\sigma_3)]\end{matrix}\right\}^m\right\} = \frac{\sigma_1 - 2v\sigma_3}{E\varepsilon_1} \tag{16}$$

The collation and simplification gives

$$m\ln\left(\frac{E\varepsilon_1}{n(\sigma_1 - 2v\sigma_3)}[\frac{1}{\sqrt{3}}(\sigma_1 - \sigma_3) - \alpha(\sigma_1 + 2\sigma_3)]\right) = \ln\left(-\ln\frac{\sigma_1 - 2v\sigma_3}{E\varepsilon_1}\right) \tag{17}$$

Regarding the stress-strain curves of rock under compression, the peak point, or the compressive strength, is the most prominent feature. The peak point method necessitates that the statistical damage principal equation's curve, derived from the measured stresses and strains, intersects the triaxial compression test curve of the rock at the highest point, which means that the highest points of the two curves should coincide at the same strain value.

According to the shape of the stress-strain curve, the stress and strain at the peak point of the curve satisfy the following relationship.

$$\left.\frac{\partial\sigma_1}{\partial\varepsilon_1}\right|_{\sigma_1=\sigma_p} = 0 \tag{18}$$

$$\sigma_1 = \sigma_p, \varepsilon_1 = \varepsilon_p \tag{19}$$

The axial stress σ_p and axial strain ε_p are denoted at the peak point. The current study employs the peak point method to resolve the n and m parameters in Eq. (16). To accomplish this, two equations are established based on the peak condition Eq. (18) and Eq. (19), which are then utilized to deduce the values of the parameters n and m. For

a concise expression, the following substitutions are utilized.

$$\left.\begin{array}{l} f(\sigma_1,\varepsilon_1)=\dfrac{\sigma_1-2\nu\sigma_3}{E\varepsilon_1} \\ g(\sigma_1)=\sigma_1-\sigma_3 \end{array}\right\} \tag{20}$$

Substituting Eq. (20) into Eq. (17) yields

$$m\ln\left(\frac{\dfrac{g(\sigma_1)}{\sqrt{3}f(\sigma_1,\varepsilon_1)}-\alpha\dfrac{3\sigma_1-2g(\sigma_1)}{f(\sigma_1,\varepsilon_1)}}{n}\right) = \ln\left[-\ln\left[f(\sigma_1,\varepsilon_1)\right]\right] \tag{21}$$

Then the stress σ_1 on both sides of Eq. (21) is found as the first order differential partial derivative of ε_1 to obtain Eq. (22).

$$\begin{aligned} &m\frac{\sqrt{3}f(\sigma_1,\varepsilon_1)}{g(\sigma_1)-3\sqrt{3}\alpha\sigma_1+2\sqrt{3}\alpha f(\sigma_1,\varepsilon_1)}\cdot \\ &\left[\begin{array}{l}\dfrac{-\sqrt{3}f'(\sigma_1,\varepsilon_1)g(\sigma_1)}{3f^2(\sigma_1,\varepsilon_1)}- \\ \alpha\dfrac{-3\sigma_1 f'(\sigma_1,\varepsilon_1)+2g(\sigma_1)\cdot f'(\sigma_1,\varepsilon_1)}{f^2(\sigma_1,\varepsilon_1)}\end{array}\right] \\ &=-\frac{1}{\ln\left[f(\sigma_1,\varepsilon_1)\right]}\cdot(-1)\cdot\frac{1}{f(\sigma_1,\varepsilon_1)}\cdot \\ &\left[\frac{\partial\sigma_1}{\partial\varepsilon_1}f'(\sigma_1,\varepsilon_1)+f'(\sigma_1,\varepsilon_1)\right] \end{aligned} \tag{22}$$

According to Eq. (18), the both sides of the equation are simplied as

$$\frac{m}{\varepsilon_1}\cdot\frac{\sqrt{3}(\sigma_1-\sigma_3)-3\alpha(\sigma_1+2\sigma_3)}{\sqrt{3}(\sigma_1-\sigma_3)-3\alpha(\sigma_1+2\sigma_3)} =-\frac{1}{\varepsilon_1}\cdot\frac{1}{\ln\left[f(\sigma_1,\varepsilon_1)\right]} \tag{23}$$

Combining Eq. (19) with Eq. (23), It can seen that the value of m is

$$m=-\frac{1}{\ln\left[f(\sigma_1,\varepsilon_1)\right]}=-\frac{1}{\ln\left[\dfrac{\sigma_p-2\nu\sigma_3}{E\varepsilon_p}\right]} \tag{24}$$

Combining Eq. (17) with Eqs. (18) and (24), the value of n is

$$n=-\frac{E^2\varepsilon_p{}^2}{(\sigma_p-2\nu\sigma_3)^2}\left[\frac{1}{\sqrt{3}}\cdot(\sigma_p-\sigma_3)-\alpha(\sigma_p+2\sigma_3)\right]\cdot\frac{1}{\ln\left(-\ln\left[\dfrac{\sigma_p-2\nu\sigma_3}{E\varepsilon_p}\right]\right)} \tag{25}$$

3. Experiment and model validation

3.1 Experimental apparatus

The experiment employed the MTS 815 2.0 electro-hydraulic servo rock mechanics testing system. This study based on the test results, solved for the parameters m and n in the model, which were ultimately used to validate the damage constitutive model.

As shown in Fig. 1, this experiment selected two types of rock samples with different properties, namely sandstone and mudstone, from the Chen Silou Coal Mine in Yongcheng, Henan Province, China, for testing and analysis. Obtain rock specimens by coring, and fabricate them into cylindrical samples with dimensions of 50 mm×100 mm, which are then subjected to triaxial compression tests under equal confining pressure.

3.2 Preparation of sandstone samples and validation of results

3.2.1 Specific steps of the sandstone test program

Below are the steps entailed in conducting a triaxial compression experiment of sandstone:

(1) Drying rock cores: The cores were dried at 35°C for 72 hours, and then cooled in a desiccator with silica gel at the bottom.

(2) The length, diameter and mass of the rock samples are measured with a digital vernier calipers and numbered.

(3) The rock samples are submerged in water for varying intervals, i.e., 1 week, 5 months, 7 months, 1 year, and the surface cracks on the samples are continuously monitored under all four immersion environments.

(4) The rock sample is placed on the loading platform and subjected to a 1kN force to fix it in place, and then a hoop strain gage is placed in the center of the sample and connected to the strain gage and the test equipment.

(5) Operating and controlling the equipment: The circumferential pressure is applied to 10 MPa at a rate of 0.02 MPa/s, after which the displacement is zeroed.

The stress-strain curves of sandstone subjected to triaxial compression tests with different immersion times are shown in Fig. 2. It can be seen from Fig. 2, the yield strength of sandstone decreases significantly with the increase of water immersion time. The yield strength of the dry rock sample is 126.3 MPa, and the yield strength of the sandstone after one week of water immersion decreases to 102.6 MPa, with a strength reduction rate of 18.8%. After five months of immersion, the yield strength decreased to 66.42 MPa, with a strength reduction rate of 47.4%. After seven months of immersion, the yield strength of the sandstone decreased to 57.4 MPa, with a strength reduction rate of 54.5%. After one year of immersion, the yield strength reached 42.6 MPa, with a strength reduction rate of 66.2%. It can be seen that the weakening effect of water on the rock is non-negligible, so it is necessary to consider the damage formed by water on the rock in the damage constitutive model.

The water content of the rock is a crucial factor influencing the compressive strength index of rocks (Dyke and Dobereiner 1991), but the water content of the rock is

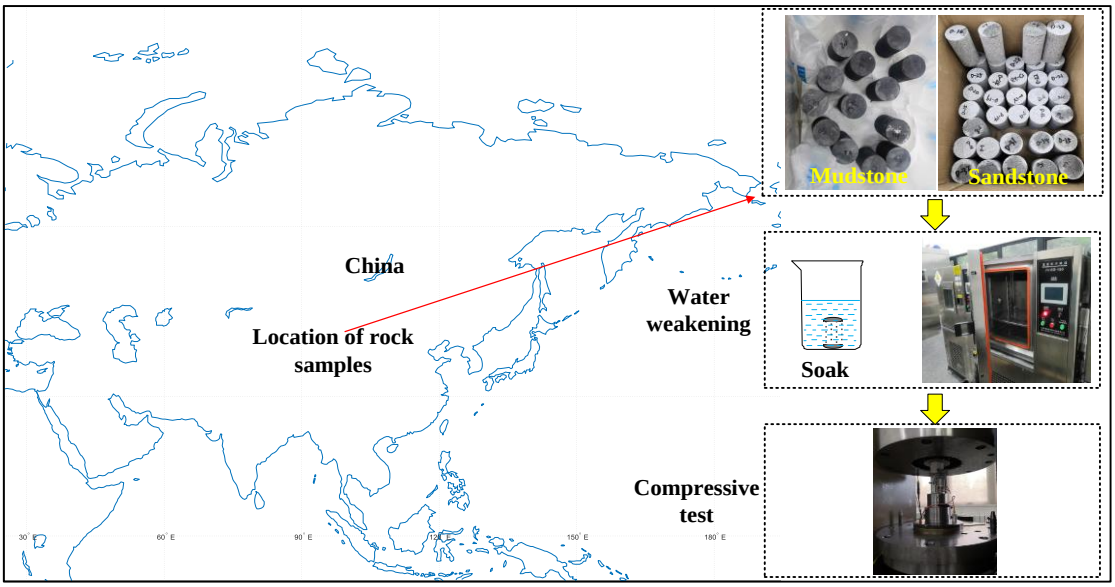

Fig. 1 Equipment and sample preparation (Modified from Wu *et al.* 2020)

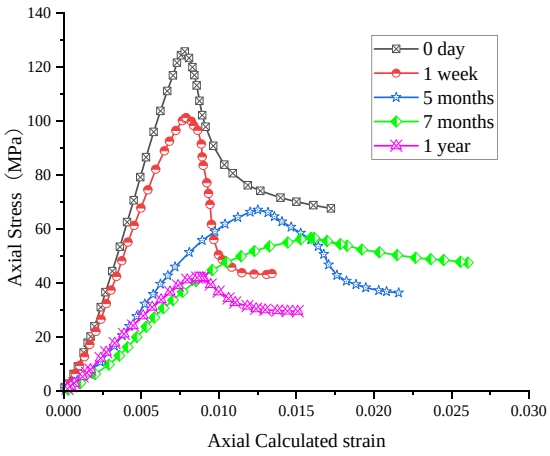

Fig. 2 Stress-strain curve of triaxial compression test for sandstone after different immersion times

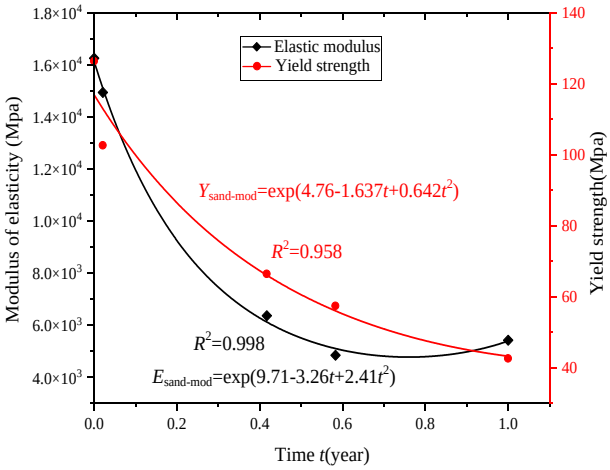

Fig. 3 Fitting curve of elastic modulus and yield strength of sandstone

not easy to determine, and it is not possible to cause significant damage to the rock in a short period of water contact, thereby yielding results that inadequately capture the true circumstances.

Therefore, in order to verify the weakening effect of water on the rock to soak the rock treatment, the effect of the rock water content on the strength of the rock can be ignored. The focus was solely on the changes in the elastic modulus of the stress-strain curve during the elastic phase relative to the immersion time. The elastic modulus and yield strength of the rock exhibit a destructive variation with soaking time, as shown in Fig. 3 The results are all exponential functions, with Eq. (26) representing the elastic modulus expression and Eq. (27) representing the yield strength expression, where t denotes the soaking time

$$E_{sand-mod} = \exp(9.71-3.26t+2.14t^2) \quad (26)$$

$$Y_{sand-mod} = \exp(4.76-1.637t+0.642t^2) \quad (27)$$

3.2.2 Damage evolution process of sandstone

Eqs. (24) and (25) were used to fit the sandstone test data shown in Fig. 2 for different confining pressures. Fig. 4 illustrates the fitting parameters of the damage constitutive model for sandstone at different times, with the expressions for parameters m and n being respectively represented by Eqs. (28) and (29).

$$Y_{sand-m} = 3.31+14.68/(1+\exp((t-0.018)/0.001)) \quad (28)$$

$$Y_{sand-n} = 58.428-40.052t+3.171t^2 \quad (29)$$

Fig. 5 illustrates the comparative stress-strain curves of experimental results and model-based predictions under various soaking times, demonstrating a strong agreement between the proposed model and experimental data across different soaking times. Fig. 6 depicts the evolution of total damage variables of sandstone under triaxial loading at different soaking times. As shown, during the initial loading stage, the inherent spatial defects of the rock material are

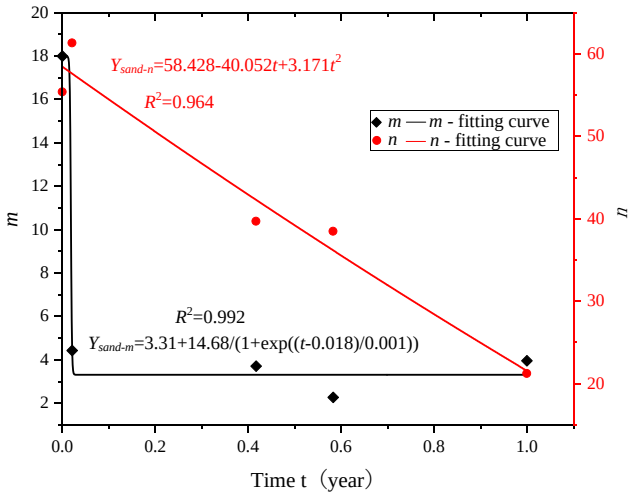

Fig. 4 Fitting parameters of the damage constitutive model for sandstone under different soaking times

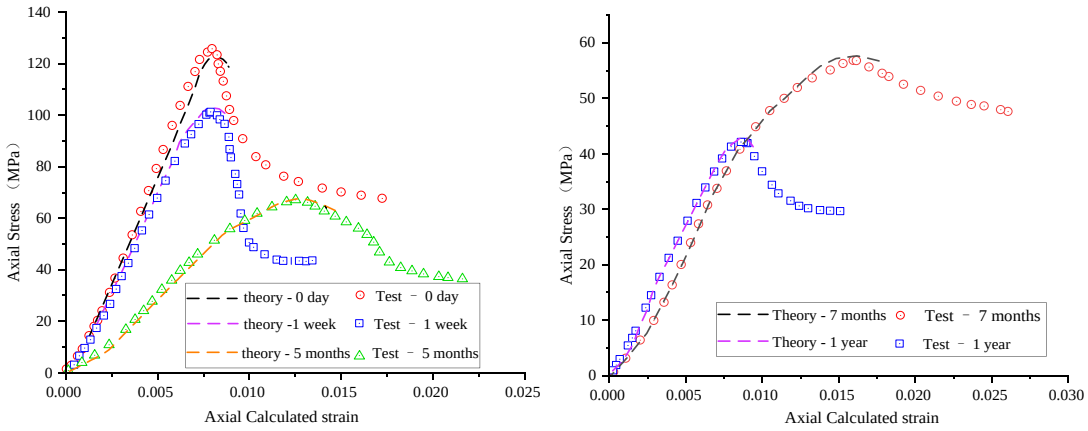

Fig. 5 Comparison of stress-strain curves for experimental and theoretical results at different immersion

gradually compacted, and the original cracks are closed, with no internal damage occurring. As the load increases, the rock enters the elastic phase, exhibiting elastic deformation; subsequently, microcracks emerge and continually expand, leading to the appearance of macroscopic cracks; finally, the rock undergoes sudden failure. Furthermore, during the experimental process, the sandstone subjected to one-year soaking exhibits more rapid damage than those soaked for five and seven months, due to the excessive weakening effect of water.

Fig. 7 provides a detailed illustration of the damage evolution curve for sandstone soaked for one week. The damage process of water-saturated sandstone can be divided into the following five stages: no damage stage (OA), minor damage increment stage (AB), rapid damage growth stage (BC), rock failure stage (CD), and rock sliding stage (DE).

During the OA stage, the initial stage of triaxial compression, the pore volume inside the sandstone sample gradually decreases, and the original microfractures close. Therefore, no new cracks form or extend, resulting in no damage. In the AB stage, the rock undergoes elastic deformation. The initial microcracks expand slowly and steadily, resulting in slow damage growth.

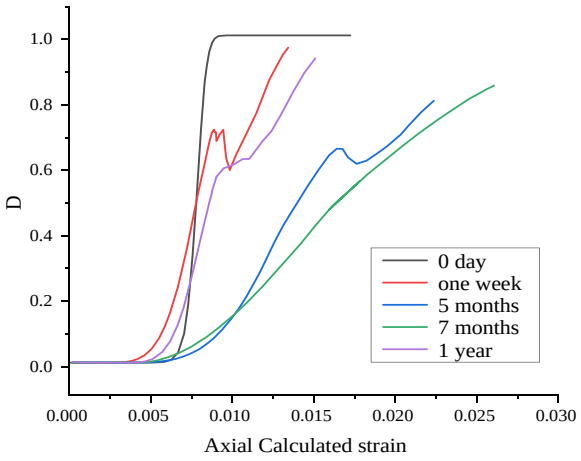

Fig. 6 Damage evolution curve of sandstone under different water immersion conditions

The BC stage is after the stress reaches a certain value. As microcracks continue to expand and connect, the damage accumulates and grows rapidly. In the CD stage, as the strain exceeds the peak, the cracks expand, the rock undergoes lateral movement, and the damage continues to

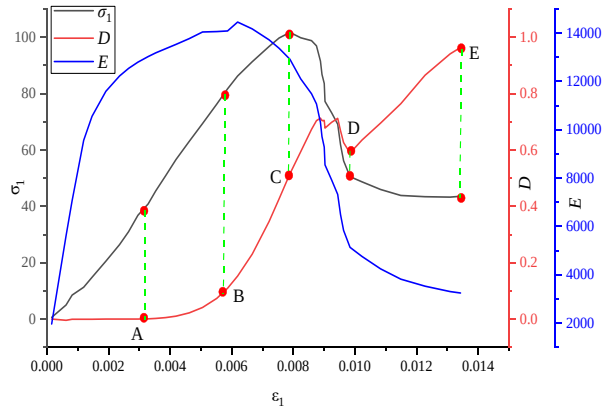

Fig. 7 Curves of $D,\sigma_1-\varepsilon_1$, E evolution process of sandstone; water-saturated sandstone for one week

Fig. 8 Evolution of crack development in mudstone under soaking (Modified from Wu *et al.* 2020)

increase. During this stage, the rock absorbs a large amount of water, which is squeezed out but remains around the rock, resulting in a slight decrease in damage, followed by continued increase. In the DE stage, the damage gradually approaches the critical value of 1, which indicates that the rock is completely damaged from a macro perspective.

3.3 Preparation of mudstone samples and validation of results

3.3.1 Specific steps of the mudstone test project

A complete rock sample is selected and then immersed in water for one month, and its fracture development was observedas shown in Fig. 8. The results show that the mudstone cracks are well developed on the surface of the rock sample, and the number of swelling fractures in the rock sample is predominant, and the rock becomes more easily broken after soaking in water, making it essential to investigate the damaging effects of water on mudstone.

The experiment utilized a temperature and humidity environmental test chamber to simulate the weakening effect of water on mudstone. The test is divided into four steps: 1) sample preparation, drying, and measurement, following the same method described in 3.2.1; 2)The temperature and humidity environmental chamber is calibrated, wherein the relative humidity is set to 80%, 60%, 40%, 20% and 0%, respectively, with a temperature of 35℃, after which the sample is placed inside the chamber and maintained in this environment for 24 hours; 3) Design the test procedure and commission the test equipment; 4) Upon completion of all experiments, the data are collated and the test results obtained.

A total of 20 rock samples were prepared for the experiment, comprising 15 test specimens (3 rock samples

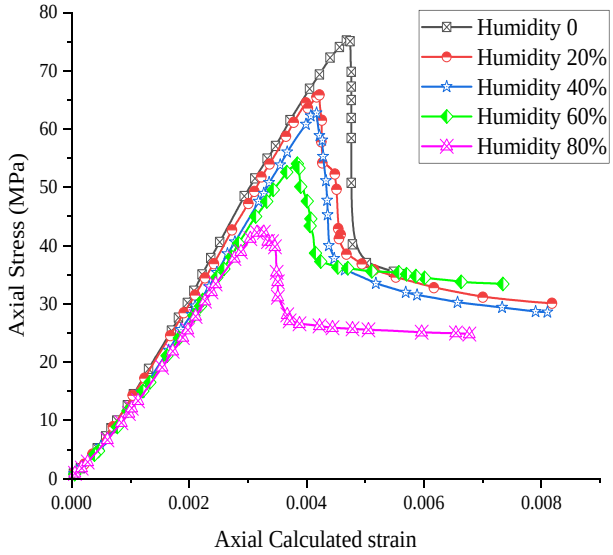

Fig. 9 Stress-strain curves of triaxial compression tests on mudstone under different humidity environments

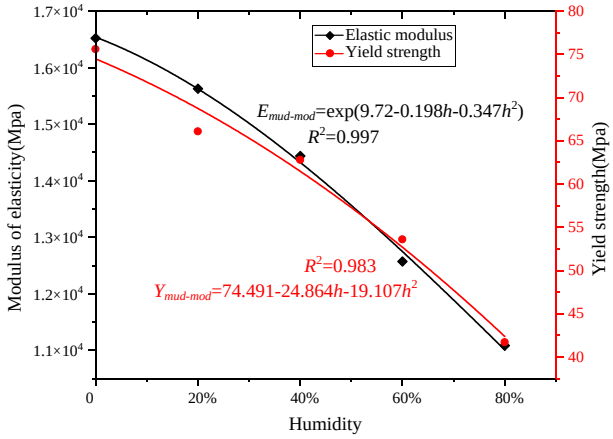

Fig. 10 Fitting curve of elastic modulus and yield strength of mudstone

per group) and 5 backup samples. During testing, rock samples were placed in the environmental box for 24 hours, and the test equipment used was the MTS 815.02 with the confining pressure setting for the test is 5 MPa, Fig. 9 presents the findings of the test.

As can be seen in Fig. 9, the weakening effect of water on mudstone is remarkably pronounced. As humidity levels rise, the yield strength of mudstone progressively declines: at 0% humidity, the yield strength is 75.6 MPa, dropping to 66.1 MPa (a reduction of 12.5%) at 20% humidity, further decreasing to 62.8 MPa (a reduction of 16.9%) at 40% humidity, and to 53.6 MPa (a reduction of 29.1%) at 60% humidity. Finally, at 80% humidity, the minimum yield strength of mudstone is 41.7 MPa, repre- senting a reduction of 44.8%. The relationship between the two can be represented by the following function

Fig. 10 indicating a significant reduction in mudstone's elastic modulus. This suggests that water has a profound impact on mudstone's elastoplasticity. The functional relationships between the rock's elastic modulus, yield

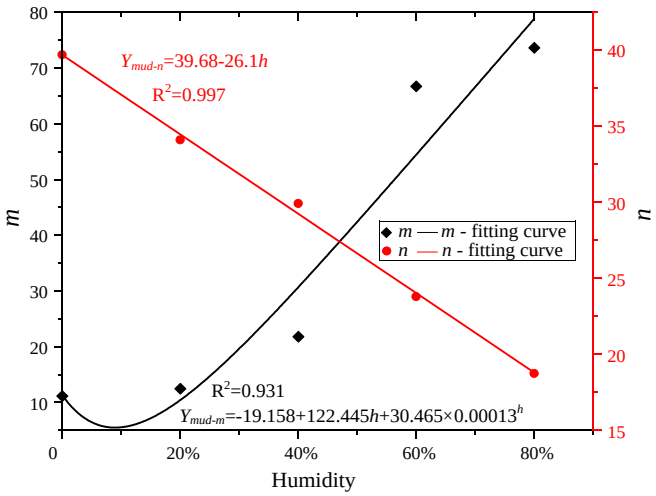

Fig. 11 Fitting parameters of the damage constitutive model for mudstone under different environmental humidity conditions

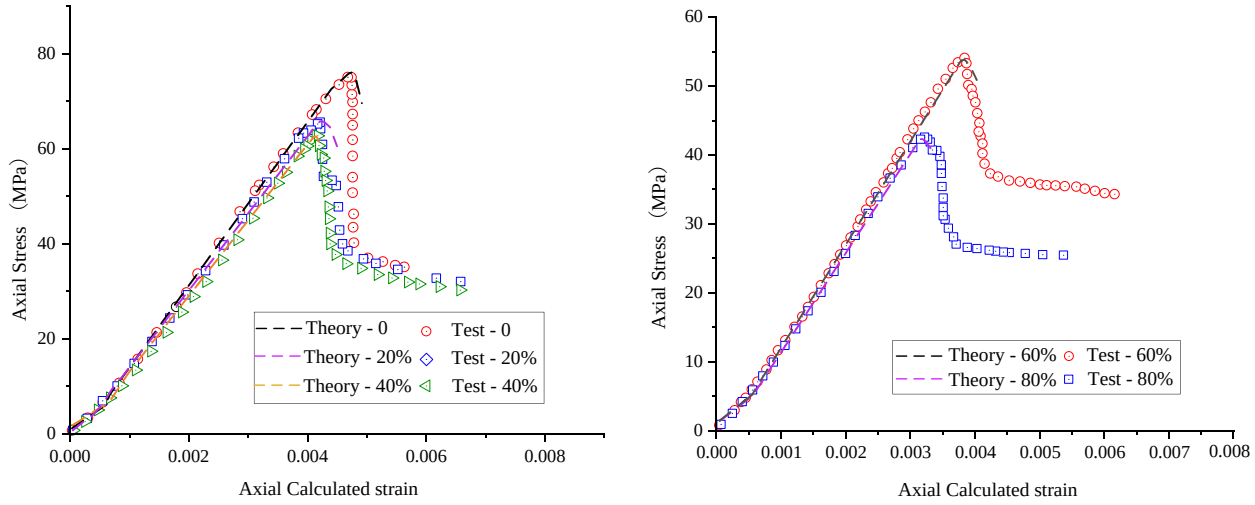

Fig. 12 Comparison of stress-strain curves for experimental and theoretical results at different environmental humidity

strength, and environmental humidity are expressed by Eqs. (30) and (31), where h denotes the environmental humidity.

$$E_{mud-\mathrm{mod}} = \exp(9.75 - 0.22h - 0.003h^2) \quad (30)$$

$$Y_{mud-mod} = 74.491 - 24.864h - 19.107h^2 \quad (31)$$

3.3.2 Evolution process of mudstone damage

Fig. 11 illustrates the fitting curves of the damage constitutive model parameters for mudstone under different environmental humidity conditions, with the expressions for m and n being respectively represented by Eqs. (32) and (33).

$$Y_{mud-m} = -19.158 + 122.445h + 30.465 \times 0.00013^h \quad (32)$$

$$Y_{mud-\mathrm{m}} = 39.68 - 26.1h \quad (33)$$

Fig. 12 illustrates the comparative analysis between theoretical and experimental curves. In general, the theoretical stress-strain curves derived from the statistical damage constitutive equation exhibit good agreement with the experimentally measured stress-strain curves obtained from the uniaxial compression tests on rocks. Fig. 13 displays the damage evolution curves of the mudstone under various environmental humidity conditions. As depictedin the figure, the damage evolution trend of mudstone can be observed.

As evident from Fig. 14, the damage evolution process of the water-immersed mudstone can also be divided into five distinct stages. During the OA stage, as the rock begins to bear the load, internal cracks are closed, and no damage is incurred. In the AB stage, the load increases gradually, resulting in minor damage to the rock sample. In the BC stage, the damage accelerates rapidly as the stress approaches the yield point. In the CD stage, due to the properties of the mudstone, the stress decreases rapidly upon reaching the peak value, while the damage continues to increase. In the DE stage, the damage continues to increase until the rock breaks.

Table 1 Assessment indicators

evaluating indicator	Calculation formula	evaluation criteria
R^2	$R^2 = 1 - \frac{\sum_{i=1}^{n}(y_i - \hat{y}_i)^2}{\sum_{i=1}^{n}(y_i - \bar{y}_i)^2}$ (a)	The closer to 1, the better
MAPE	$MAPE = \frac{100\%}{n}\sum_{i=1}^{n}\left\|\frac{y_i - \hat{y}_i}{y_i}\right\|$	The smaller the better
MAE	$MAE = \frac{1}{n}\sum_{i=1}^{n}\|y_i - \hat{y}_i\|$	The smaller the better
RMSE	$RMSE = \sqrt{\frac{1}{n}\times\sum_{i=1}^{n}(y_i - \hat{y}_i)^2}$	The smaller the better
MSE	$MSE = \frac{1}{n}\times\sum_{i=1}^{n}(y_i - \hat{y}_i)^2$	The smaller the better

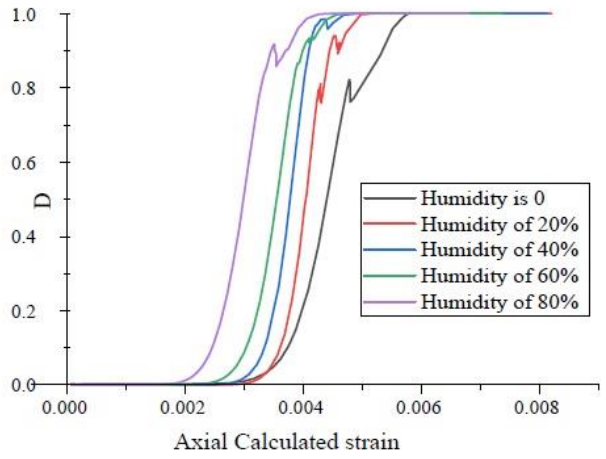

Fig. 13 Damage evolution curve of mudstone

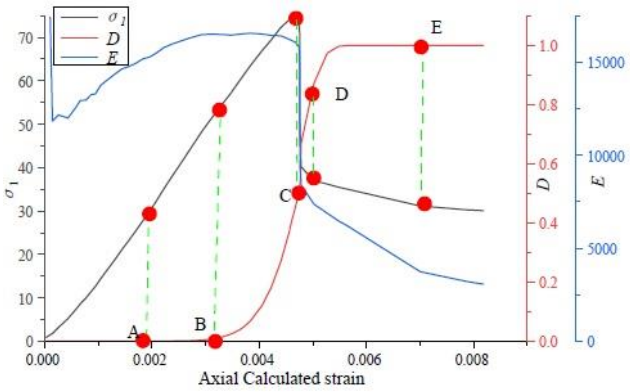

Fig. 14 Evolutionary curves of D, σ_1-ε_1, and E for mudstone

4. Results and discussion

4.1 Analysis of results

To accurately assess the reliability of a model, a multi-index comprehensive evaluation approach can be employed, involving a systematic analysis of the model's results in terms at different ambient humidity of fitting degree, predictive error, and precision. Specifically, a range of statistical parameters, such as coefficient of determination (R^2), mean absolute percentage error (MAPE), root mean squared error (RMSE), mean squared error (MSE), and mean absolute error (MAE), can be utilized to comprehensively evaluate the performance of a model or algorithm. R^2 can be used to assess the model's fitting degree to the data, measuring its explanatory and predictive capabilities; MAPE can be employed to evaluate the model's predictive error, measuring its predictive accuracy; while MSE, RMSE, and MAE can be used to assess the model's predictive error, measuring its predictive accuracy and stability. Due to data issues, only R2 before the peak of the theoretical and experimental curves was calculated in this study.The formula for calculating the assessment indicators is shown in Table 1.

As evident from Fig. 15, a strong correlation exists between the experimental and theoretical data, with R^2 values spanning 0.962 to 0.996, indicative of a high degree of consistency between the experimental results and theoretical calculations.MAPE values lie within the range of 3.589% to 9.166%, suggesting a relatively modest error magnitude.

MAE, RMSE and MSE are all relatively small, underscoring a strong fit between the experimental data and theoretical calculations. Moreover, the analysis reveals that the computational model is capable of accurately capturing the behavior of rocks under varying soaking times and humidity conditions, thereby demonstrating its efficacy and reliability in predicting rock behavior under diverse soaking times and environmental humidity.

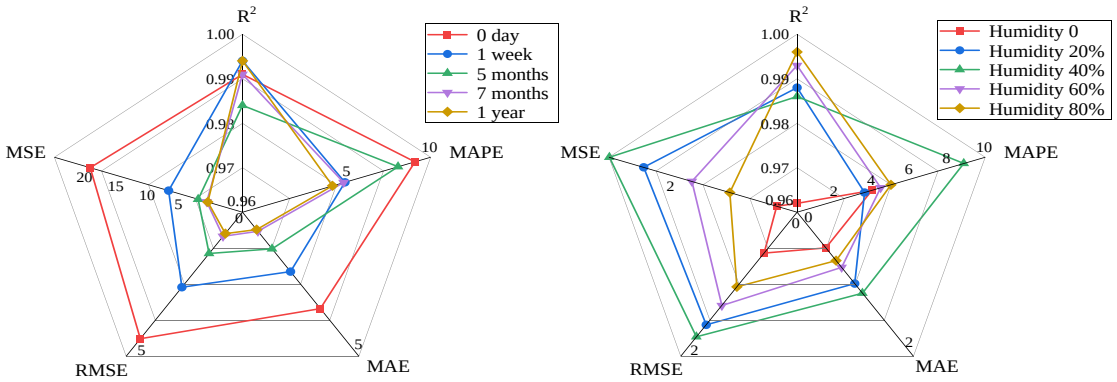

Fig. 15 Radar chart of assessment indicators

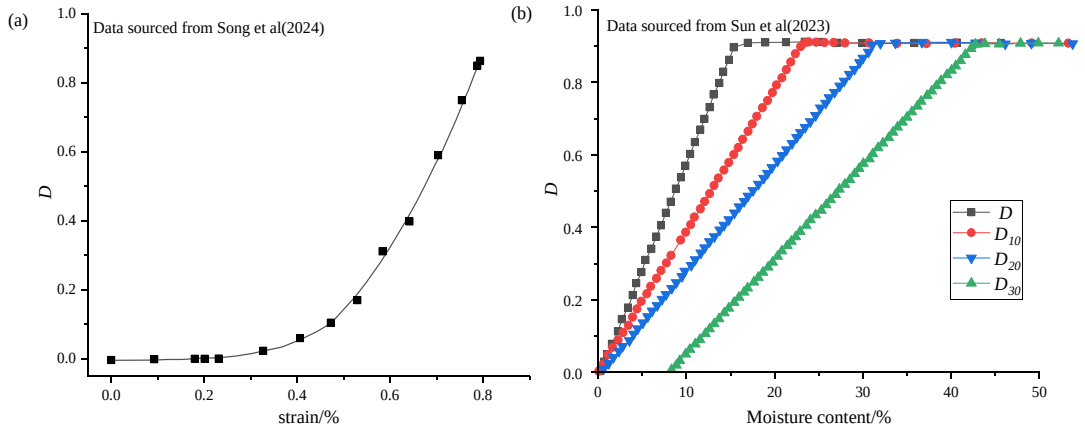

Fig. 16 Damage evolution curve of other papers

4.2 Discussion

To further elucidate the model's performance, a comparative analysis with other studies is conducted, yielding the following results:

Song *et al*. (2024) investigated the damage evolution characteristics of muddy siltstone in different water content states, and Sun *et al.* (2023) observed the weakening effect of different water contents on sandstone through triaxial compression tests, and the damage curves are shown in Fig. 16. In this study, the damage evolution curve shows a "Z" shape, as shown in Fig. 10, compared with Fig. 16(b), considering the compaction stage of the rock, the internal cracks are closed, no damage occurs, and the damage is initially zero, and this paper establishes a complete damage evolution process by considering the sliding stage of rock damage (compared with Fig. 16(a)). The evolution curve is more telling because it shows the complete damage evolution within the rock.

Numerous researchers have investigated the weakening rules of rocks under water-rock interaction through water content studies (Meng *et al*. 2009, jiang *et al*. 2009), and their research findings have deepened our under- standing of the influence of water content and water state on the physical and mechanical parameters of rocks. However, determining the water content of rocks is a complex task, and therefore, this study adopts soaking time and environmental humidity as variables to investigate the weakening effect of water on rocks.

Previous studies on the damaging effects of water on rocks have focused on the weakening effects of water content (Li *et al*. 2023), wet and dry cycles (Deng *et al.* 2017), etc. on rocks. However, in engineering practice, the rock layer in direct contact with the aquifer will always be in a water-bearing environment, or the coal seam mining leads to the development of fissure zones into the aquifer, which makes the rock be soaked by water for a long time. Therefore, this paper adopts the method of different soaking time for sandstone and different environmental humidity for mudstone to study the weakening effect of water on rock, which is more in line with the mining engineering background.

5. Conclusions

To address rock instability and failure caused by water weakening, the weakening mechanism of water on rock is discussed, and a statistical damage constitutive equation is established in this study. The main conclusions drawn are as follows:

The rock's compressive strength relationship with soaking time follows an exponential function form. After one year of water immersion, the strength of sandstone decreases by 66%, and the strength of mudstone decreases by 44.8% after 24 hours in an 80% humidity environment. Moreover, the rock's elastic modulus displays a nonlinear decay trend with increasing soaking time and environmental humidity.

A statistical damage model for water-weakened rocks was proposed, which employed the Weibull distribution function to describe the discrete mechanical properties of rock elements and the D-P yield criterion to describe the strength of rock elements. The theoretical calculation results for sandstone and mudstone exhibit a good fit, with R^2 values ranging from 0.962 to 0.996. Moreover, the MAPE,MAE, MSE, and RMSE values are also relatively low, indicating that the model possesses high accuracy and reliability.

The damage evolution curve can be roughly divided into five different stages. I satge: the pore volume decreases, the original microcracks are sealed, and no damage occurs. II stage: as the load gradually increases, the damage progressively intensifies, which aligns with the evolution of the elastic modulus, with only minor damage. III stage: as the stress approaches the yield point, the accumulation of damage accelerates until rock failure ensues. IV stage: After reaching the peak point, the damage continues to increase, with cracks further expanding. V stage: the damage continues to accumulate until the rock is completely destroyed. The macroscopic crack network and microscopic cracks are visible.

This study has made a preliminary attempt to develop a rock constitutive model that takes into account the weakening effect of water, with results indicating a good fit between experimental and theoretical curves. However, the research still has certain limitations. The proposed model may lack accuracy in engineering applications due to the complex stress state and loading process of in-situ rocks, including effects of separate layers of water, water pressure, and temperature changes. Future research should consider these factors to develop a more realistic and applicable model for mining engineering.

Acknowledgments

All authors contributed to the study conception and design. This work is supported by Henan Natural Science Foundation Youth Fund Project (No.232300421331),Key Scientific Research Projects of Colleges and Universities in Henan Province (No.23A440005) and Postdoctoral Research Grant in Henan Province (No.202103049), China Postdoctoral Science Foundation (2023M741009).

References

Bian, K., Liu, J., Zhang, W., Zheng, X., Ni, S. and Liu, Z. (2019), "Mechanical behavior and damage constitutive model of rock subjected to water-weakening effect and uniaxial loading", *Rock Mech. Rock Eng.*, **52**(1), 97-106. https://doi.org/10.1007/s00603-018-1580-4.

Cai, X., Zhou, Z., Liu, K., Du, X. and Zang, H. (2019), "Water-weakening effects the on mechanical behavior of different rock types:Phenomena and mechanisms", *Appl. Sci.*, **9**(20). https://doi.org/10.3390/app9204450.

Cao, W.G., Fang, Z.L. and Tang, X.J. (1998), "Research on statistical constitutive models for rock damage and softening", *J. Rock Mech. Eng.*, **17**(6):628-633.

Chen,Y., Xiao, P., Du, X., Wang, S., Fernandez-Steeger, T.M. and Azzam, R. (2021), "Study on damage constitutive model of rock under freeze-thaw-confining pressureacid erosion", *Appl. Sci.*, **11**(20), 9431. https://doi.org/10.3390/APP11209431

Deng, H., Hu, A., Li, J., Zhang, X., Hu, Y., Chang, D. and Zhu, D. (2017), "Statistical constitutive model for sandstone degradation and damage under water rock interaction", *Geotech. Mech.*, **38**(3), 631-639. https://doi.org/10.16285/j.rsm.2017.03.003.

Dyke, C.G. and Dobereiner, L. (1991), "Evaluating the strength and deformability of sandstones", *Int. J. Rock Mech. Min. Sci. Geomech. Abstracts,* **28**(1), 123-134. https://doi.org/10.1144/GSL.QJEG.1991.024.01.13.

Feng, X.T., Chen, S. and Li, S. (2001), "Effects of water chemistry on microcracking and compressive strength of granite - sciencedirect", *Int. J. Rock Mech. Min. Sci.s*, **38**(4), 557-568. https://doi.org/10.1016/S1365-1609(01)00016-8.

He, Z., Zhu, Z., Ruan, H. and Dai, B. (2019), "Research on statistical damage constitutive model of rock under water pressure", *J. Yangtze River Academy Sci.,* **36**(6), 6. https://doi.org/10.11988/ckyyb.20171328.

Huang, X., Yang, C., Liu, J., He, X., Chen, J. and Duan, X. (2008), "Creep tests of mudstone under different water content conditions and their impact on casing damage in oil fields", *J. Rock Mech. Eng.*, **27**(2), 3477–3482. https://doi.org/10.3321/j.issn:1000-6915.2008.z2.026.

Jean Lemaitre, T.B.N.J. and Chunhu, T. (1996), Damage mechanics Course, Science Press, Beijing, China.

Jiang, J., Hou, Z.M., Hou, K.P., Lu, Y.F., Sun, H.F. and Niu, X.D. (2009), "The damage constitutive model of sandstone under water-rock coupling", *J. Rock Mech. Eng.*, **28**(1), 2637-2643. https://doi.org/10.3321/j.issn:1000-6915.2009.z1.007.

Kim, E., Stine, M.A., de Oliveira, D.B.M. and Changani, H. (2017), "Correlations between the physical and mechanical properties of sandstones with changes of water content and loading rates", *Int. J. Rock Mech. Min. Sci.*, **100**, 255-262. https://doi.org/10.1016/j.ijrmms.2017.11.00595.

Krajcinovic, D. and Silva, M.A.G. (1982), "Statistical aspects of the continuous damage theory", *Int. J. Solids Struct.*, **18**(7): 551-562. https://doi.org/10.1016/0020-7683(82)90039-7.

Li, T., Chen, Z., Chen, G., Ma, C., Tang, O. and Wang, M. (2015), "Research on the energy mechanism of sandstone under different water content effects", *Geotech. Mech.*, **36**(2), 229-236. https://doi.org/10.16285/j.rsm.2015.S2.030.

Li, X., Che, X., Li, H. and Qi, C. (2023), "A meso-macro method of evaluating water content effect on direct tensile fracture in brittle rocks", *KSCE J. Civil Eng.*, **28**(4), 1513-1521. https://doi.org/10.1007/S12205-023-0255-1.

Li, Z., Liu. S., Ren. W., Fang, J., Zhu, Q. and Dun, Z. (2020), "Multiscale laboratory study and numerical analysis of water-weakening effect on shale", *Adv. Mater. Sci. Eng.*, **2020**(7), 1-14. https://doi.org/10.1155/2020/5263431.

Liu, B., Yu, M., Sun, J., Huang, R. and Deng, T. (2023), "Study on mechanical properties and damage constitutive model of shale under water force coupling cooperation", *J. Rock Mech. Eng.*, **42**, 1-14. https://doi.org/10.13722/j.cnki.jrme.2022.0655.

Liu, J., Zhu, X., Xu, L. and Zhang, S. (2021), "Study on the damage evolution law of granite after high temperature cooling", *Coal Technology*, **40**(2), 30-33. https://doi.org/10.13301/ j. cnki.ct.2021.02.009.

Ma, D., Cai, X., Li, Q. and Duan, H. (2018), "In-situ and numerical investigation of groundwater inrush hazard from grouted karst collapse pillar in longwall mining", *Water*, **10**(9): 1187-1187. https://doi.org/10.3390/w10091187.

Ma, T., Yang, C., Chen, P., Wang, X. and Guo, Y. (2016), "On the damage constitutive model for hydrated shale using ct scanning technology", *J. Natural Gas Sci. Eng.*, **28**, 204-214. https://doi.org/10.1016/j.jngse.2015.11.025.

Meng, Z., Pan, J., Liu, L., Meng, G. and Zhao, Z. (2009), "The influence of water content on the mechanical properties and impact tendency of sedimentary rocks", *J. Rock Mech. Eng.*, **28**(1), 2637-2643. https://doi.org/10.3321/j.issn:1000-6915.2009.z1.007.

Miao, F., Wu, Y .,Ákos T , Li, L. and Xue, Y. (2022), "Centrifugal model test on a riverine landslide in the Three Gorges Reservoir induced by rainfall and water level fluctuation", *Geosci. Front.*, **13**(3), 101378. https://doi.org/10.1016/j.gsf.2022.101378.

Mousavi S, Tavakoli H, Moarefvand P. and Rezaei, M. (2020a), "Evaluating the effect of freezing-thawing cycles on the compressional wavevelocity and dry density of schist rock (case study: Angouran mine)", *Appl. Geol.*, **10**(2020), 15-30. https://doi.org/10.22055/AAG.2019.28197.1922.

Mousavi, S.Z.S. and Rezaei, M. (2022), "Correlation assessment between degradation ratios of ucs and non-destructive properties of rock under freezingthawing cycles", *Geoderma*, **428**(116209). https://doi.org/10.1016/j.geoderma.2022.116209.

Mousavi, S.Z.S., Tavakoli, H., Moarefvand, P. and Rezaei, M. (2019), "Assessing the effect of freezing-thawing cycles on the results of the triaxial compressive strength test for calc-schist rock", *Int. J. Rock Mech. Min. Sci.*, **123**, 104090. https://doi.org/10.1016/j.ijrmms.2019.104090.

Mousavi S.Z.S., Tavakoli, H., Moarefvand, P. and Rezaei, M. (2020b), "Micro-structural, petro- graphical and mechanical studies of schist rocks under the freezingthawing cycles", *Cold Reg. Sci. Technol.*, **174**(103039). https://doi.org/10.1016/j.coldregions.2020.103039.

Olena S. (2019), "Water effect on the rocks and mine roadways stability" *E3S Web of Conferences*, **109**, 1-7. https://doi.org/10.1051/e3sconf/201910900092.

Pan, J.L., Cai, M.f., Li, P. and Guo, Q. (2022), "A damage constitutive model of rock-like materials containing a single crack under the action of chemical corrosion and uniaxial compression", *J. Central South Univ.*, **29**, 1-13. https://doi.org/10.1007/S11771-022-4949-1.

Peng, Y. (2018), "Research on statistical constitutive model of rock damage under triaxial compression", *Technol. Innov. Appl.*, (24), 2. https://doi.org/CNKI:SUN:CXYY.0.2018-24-017.

Qi, X., Tian, A., Luo, X., and Tang, Q. (2022), "Chemical damage constitutive model establishment and the energy analysis of rocks under water–rock interaction", *Energies*, **15**(24), 9386-9386. https://doi.org/10.3390/EN15249386.

Qin, Y. (2001), "Discussion on damage mechanics model of rock and its constitutive equation", *J. Rock Nech. Eng.*, **20**(4), 3. https://doi.org/10.3321/j.issn:1000-6915.2001.04.028.

Rabotnov, Y.N. (1963), "On the equations of state for creep", *Progress Appl. Mech.*, **178**, 307-315.

Seyed Mousavi, S.Z., Tavakoli, H., Moarefvand, P. and Rezaei, M. (2020), "Evaluating the variations of density and durability index of schist rock under the effect of freezing-thawing cycles", *Iranian Soc. Min. Eng.*, **14**(45), 1-12. https://doi.org/10.22034/IJME.2020.37382.

Shi, W., Cai, W., Meng, Y., Li, G., Wnn, K. and Zhang, Y. (2016), "Weakening laws of rock uniaxial compressive strength with consideration of water content and rock porosity", *Arabian J. Geosci.*, **9**(5), 369-369. https://doi.org/10.1007/s12517-016-2426-6.

Song, H., Li, S., Zhang, Q., Guo, Y. and Xu, G. (2024), "A study on the characteristics of acoustic emission stage and damage evolution of cement containing sandstone", *J. Undergr. Sp. Eng.*, **20**(1), 72-81.

Sun, B., Yang, H., Zeng, S., Yin, Y. and Fan, J. (2023), "Crack initiation mechanism and meso- crack evolution of pre-fabricated cracked sandstone specimens under uniaxial loading", *Geomech. Eng.*, **33**(6), 597-609. https://doi.org/10.12989/gae.2023.33.6.597.

Sun, Z., Zhang, Q., Ju, Z., Zhang, Y. and Wang, P. (2023b), "A study of constitutive model of rock damage under the joint effect of load and moisture", *Appl. Sci.*, **13**(2). https://doi.org/10.3390/APP13021224.

Wang, S., Qi, X., Fu, P., *et al.* (2022), "Study on constitutive relationship of composite rock considering temperature damage", *Min. Res. Development*, **42**(12), 8. https://doi.org/10.13827/j.cnki.kyyk.2022.12.012.

Wang, Y., Liu, X., Liang,, L. and Ziong, J. (2020), "Experimental study on the damage of organic-rich shale during water-shale interaction", *J. Natural Gas Sci. Eng.*, **74**, 103103. https://doi.org/10.1016/j.jngse.2019.103103.

Wasantha, P. and Ranjith, P. (2014), "Water-weakening behavior of hawkesbury sandstone in brittle regime", *Eng. Geol.*, **178**, 91-101. https://doi.org/10.1016/j.enggeo.2014.05.015.

Wong, F. (2013), "Research on rock statistical damage constitutive model based on triaxial compression test", MS, Tsinghua University, Beijing.

Wu, L. (2020), "Research on the evolution mechanism of water inrush disasters in coal seam overlying strata", PhD thesis, China University of Mining and Technology, Xuzhou. 10.27623/d.cnki.gzkyu.2020.001832.

Wu, Z., Ji, X., Liu, Q. and Fan, L. (2020), "Study of microstructure effect on the nonlinear mechanical behavior and failure process of rock using an image-based-fdem model", *Comput. Geotech.*, **121**, 103480. https://doi.org/10.1016/j.compgeo.2020.103480.

Xie, H., Li, X., Shan, C., Xia, Z. and Yu, L. (2022), "Study on the damage mechanism and energy evolution characteristics of water-bearing coal samples under cyclic loading", *Rock Mech. Rock Eng.*, **56**(2), 1367-1385. https://doi.org/10.1007/S00603-022-03136-8

Xu, W. and Wei, L. (2002), "Research on statistical constitutive models for rock damage", *J. Rock Mech. Eng.*, **21**(6), 5. https://doi.org/10.3321/j.issn:1000-6915.2002.06.006.

Yang, X. and Jiang, A. (2022), "Study on the coupled mechanism of seep-age–stress damage and damage constitutive model of rock after freezing and thawing", *Int. J. Geomech.*, **22**(11). https://doi.org/10.1061/(ASCE)GM.1943-5622.0002402.

Yang, Y. (2011), "Critical warning characteristics of water inrush geological hazards in karst tunnels", PhD thesis, Beijing Jiaotong University, Beijing.

Zhai, Y., Meng, F., Li, Y., Zhao, R. and Zhang, Y. (2022), "Research on dynamic compression failure characteristics and damage constitutive model of sandstone after freeze–thaw cycles", *Eng. Fail. Anal.*, **140**, 106577. https://doi.org/10.1016/j.engfailanal.2022.106577.

Zhang, C., Cao, P., Wang, Y. and Ning, G. (2013), "Creep characteristics of deep amphibolite under natural and saturated conditions", *J. Central South Univ. (Natural Science Edition)*, **44**(4), 1587-1595. https://doi.org/CNKI:SUN:ZNGD.0.2013-04-043.

Zhang, C., Bai, Q., Han, P., Wnag, L., Wang, X. and Wnag, F. (2023), "Strength weakening and its micromech- anism in water–rock interaction, a short review in laboratory tests", *Int. J. Coal Sci. Tech.*, **10**(1). https://doi.org/10.1007/S40789-023-00569-6.

Zhang, Y., Wu, X., Guo, Q., Wang, L., Wang, X. and Wang, F. (2022), "Research on the mechanical properties and damage constitutive model of multi-shape fractured sandstone under hydro-mechanical coupling", *Minerals*, 12. https://doi.org/10.3390/min12040436.

Zhou, J., Lou, J., Wei, J., Dai, F., Chen, J. and Zhang, M. (2023), "A 3d microseismic data-driven damage model for jointed rock mass under hydro-mechanical coupling conditions and its application", *J. Rock Mech. Geotech. Eng.*, **15**(4), 911-925. https://doi.org/10.1016/J.JRMGE.2022.10.002.